



The first firn core from Peter 1st Island – capturing climate variability across the Bellingshausen Sea

Elizabeth R. Thomas¹, Dieter Tetzner¹, Bradley Markle^{2,3}, Joel Pedro^{4,5}, Guisella Gatacua⁶, Dorothea E. Moser^{1,7}, Sarah Jackson⁸

5 ¹Ice Dynamics and Paleoclimate, British Antarctic Survey, High Cross, Madingley Road, Cambridge, CB23 7XT, UK

²Department of Geological Sciences, University of Colorado, Boulder, USA

³Institute of Arctic and Alpine Science, University of Colorado, Boulder, USA

⁴Australian Antarctic Division, Kingston, Tasmania, 7050, Australia

10 ⁵Australian Antarctic Program Partnership, Institute for Marine and Antarctic Studies, University of Tasmania, Hobart, Tasmania, 7004, Australia

⁶National Centre for Climate Research, Danish Meteorological Institute, Copenhagen, Denmark

⁷Department of Earth Sciences, University of Cambridge, Cambridge CB2 3EQ, UK

⁸Research School of Earth Sciences, Australian National University, Canberra, ACT 2600 Australia

15

Correspondence to: Elizabeth R. Thomas (lith@bas.ac.uk)

Abstract. Peter 1st Island is situated in the Bellingshausen Sea, a region that has experienced considerable climate change in recent decades. Warming sea surface temperatures and reduced sea ice cover have been accompanied by warming surface air temperature, increased snowfall, and accelerated mass loss over the adjacent ice sheet. Here we present data from the first firn core drilled on Peter 1st Island, spanning the period 2001-2017 CE. The stable water isotope data capture regional changes in surface air temperature, and precipitation (snow accumulation) at the site, which are highly correlated with the surrounding Amundsen-Bellingshausen Seas, and the adjacent Antarctic Peninsula ($r > 0.6$, $p < 0.05$). The unique in-situ data from an automatic weather station, together with the firn core data, confirms the high skill of the ERA5 reanalysis in capturing daily mean temperature and inter-annual precipitation variability, even over a small Sub-Antarctic Island. This study demonstrates the suitability of Peter 1st Island for future deep ice core drilling, with the potential to provide an invaluable archive to explore ice-ocean-atmosphere interactions over decadal to centennial timescales for this dynamic region.

30 1. Introduction:

The Sub-Antarctic Island of Peter 1st (Peter I Øy) is a former shield volcano (154 km²), almost completely covered by a heavily crevassed ice cap. The islands' location in the Bellingshausen Sea, and just 450 km from the coast of West Antarctica, make it a scientifically important site for paleoclimate, ice sheet and oceanographic studies. The island is situated within the seasonal sea ice zone, in a region of the Southern Ocean that has experienced a rapid decline in sea ice cover in recent decades reaching a record low in February 2023 (NSIDC, 2023). The rate of sea ice decline in the Bellingshausen Sea since 1979 is comparable to the rate of ice loss in the Arctic (Parkinson, 2019). Reconstructions from ice cores suggest this recent change is part of a 20th century decline, evident in both proxy and observational based reconstructions (Abram et al., 2010; Porter et al., 2016; Thomas et al., 2019).

40 The closest landmass is the Antarctic Peninsula (AP) and Ellsworth Land coast, a region that has experienced considerable climate and glaciological change during the 20th century. Surface air temperatures on the AP, recorded at coastal research stations, have increased by as much as 2.5°C since the 1950s (Turner et al., 2005) constituting the largest warming in the Southern Hemisphere (Siegert et al., 2019). Despite a pause in the trend during the 21st century (Turner et al., 2016) warming has resumed to record levels (González-Herrero et al.,



45 2022) and paleoclimate archives suggest the warming during the late 20th century was part of a 100-year trend (Royles et al., 2013; Thomas et al., 2009; Thomas. and Tetzner., 2018), that is likely to continue in the future (Li et al., 2018). In addition to the rise in temperature, snowfall has increased dramatically during the 20th century (Thomas et al., 2015; Thomas et al., 2008; Thomas et al., 2017) attributed to changes in atmospheric circulation, sea ice changes and rising surface air temperature (Goodwin et al., 2016; Medley and Thomas, 2019; Porter et al., 2016).

Glaciers along the Bellingshausen Sea and Ellsworth Land coast have retreated in recent decades; (Paolo et al., 2015; Pritchard et al., 2009; Smith et al., 2020). Many glaciers display dynamic thinning and grounding-line retreat that has been attributed to incursions of circumpolar deep water (CDW). The water in the Bellingshausen Sea is amongst the warmest in the Southern Ocean, with measured CDW temperature exceeding 1°C (Jenkins and Jacobs, 2008). The island is situated to the northwest of the Belgica Fan, the culmination of the Belgica Trough, an exceptionally large paleo-ice stream. Ice sheet reconstructions suggest that during the last Glacial Maximum all the modern drainage basins along the Bellingshausen Sea coast were tributaries for a single large ice stream that may have extended to the continental shelf, less than ~200 km from Peter 1st Island. Thus, the location of Peter 1st Island, at the northern edge of the continental shelf, is of significance for both modern and paleoclimate, oceanographic and ice sheet studies.

The first firm core from Peter 1st Island was drilled as part of the Sub-Antarctic Ice Core Expedition (SubICE), one of the projects of the international Antarctic Circumnavigation Expedition (ACE) 2017–2018 (Walton, 2018; Thomas et al., 2021). The aim of this study is to present the chemical and stable water isotope data from the Peter 1st Island ice core to determine its suitability for paleoclimate reconstructions. In addition, we utilise a short instrumental record from an automatic weather station (AWS) from Peter 1st island to determine the skill of the ERA5 reanalysis data. We will 1) establish the firm core age-scale, 2) evaluate the skill of ERA5 at this island, 3) evaluate the firm core proxies against meteorological parameters from ERA5 and 3) discuss the suitability of this site for future deep ice core drilling.

70 **2. Data and methods:**

2.1. Ice core site



75 **Figure 1: Location of Peter 1st Island (Peter I Øy) in the Bellingshausen Sea, with the ice core site (blue rectangle) with closest Antarctic Peninsula research stations (red circles) and the Ellsworth Land ice core location referenced in the text (Ferrigno, red box). Insert map showing the Peter 1st drilling location (red box), AWS (green dot) and island topography. Map produced using the Antarctic Digital Database, using data made available under the Creative Commons Attribution 4.0 International (CC BY 4.0) licence.**

In February 2017 a shallow ice core was drilled to a depth of 12.29 m on Peter 1st Island (68°51'05" S, 90°30'35" W). A site had been selected, based on satellite imagery, at the plateau at the top of the island (Lars



80 Christentoppen), however heavy cloud cover prevented helicopter landing at this site. Instead, a lower elevation site was found on a ridge (Midtryggen) at 730 m above sea level, in a small saddle on the eastern side of the island overlooking the main glacier Storfallet (Fig. 1). The snow surface was relatively smooth at this site (slope of $\sim 5^\circ$), and ground penetrating radar (GPR) surveys were conducted in a ~ 500 m radius from the drill site (Thomas et al., 2021). Near continuous stratified layers were observed in the GPR profiles for the upper 14 m of
85 snow. The maximum time window for the GPR was set at ~ 43 m and bedrock was not detected at this depth, however, the full ice thickness has not been determined.

The firm core was drilled using a motorized Kovacs ice-core drill (Mark II) powered by a 4-stroke Honda generator, with core retrieval aided by a sidewinder winch. Ice core sections, with a maximum length of 80 cm, were stored in ethylene-vinyl-acetate-treated (EVA) polythene bags in insulated boxes.

90 The length and weight of each firm core fragment was measured to calculate density. Based on the measured density profile, and the Herron-Langway model, the estimated bubble close-off depth (when the firm air passages become closed at a density of 0.83 kg m^{-3}) is 34.5 m at this site. Visible melt layers >1 mm thick were recorded (Thomas et al., 2021), revealing an estimated 11% of the ice core is affected by melt, comparable to other Sub-Antarctic and coastal Antarctic ice core sites (Thomas et al., 2021), but considerably less than the Young Island ice core (Moser et al., 2021). Discrete samples were cut at 5 cm resolution for ion-chromatographic (IC) and
95 stable water isotope analysis, sealed in tritan copolyester jars.

2.2. Meteorological data

Meteorological data come from the European Centre for Medium-Range Weather Forecasts (ECMWF) ERA5 analysis (1979–2017) (Copernicus Climate Change Service, 2017), the fifth generation of ECMWF reanalysis.
100 ERA5 reanalysis currently extends back to 1950, providing hourly data at 0.25° resolution (~ 31 km). However, we note that the resolution of ERA5 may not fully capture local climate and precipitation on Peter 1st Island. An automatic weather station was located on the island between February 2006 and January 2007 (<http://amrc.ssec.wisc.edu/aws/index.php?region=Ocean%20Islands&station=Peter%20I&year=2006>, data downloaded 03/11/2020) providing a short (but incomplete) in-situ record of surface temperature (Thomas et al.,
105 2021). This data was not assimilated into the ECMWF model (de Rosnay, 2018). The AWS was located near $68^\circ 46.2\text{S}$, $90^\circ 30.3\text{W}$, at a height of ~ 128 m on the 'Radiosletta' Plateau on the NW side of the island (Fig.1, insert map). We utilise the observation-based Southern Hemisphere Annular Mode (SAM) Index of (Marshall, 2003) and the Southern Oscillation Index (SOI, defined as the normalized pressure difference between Tahiti and Darwin) of (Ropelewski and Jones, 1987).

2.3. Stable water isotopes

Isotopes, $\delta^{18}\text{O}$ and δD , were measured using a Picarro L2130-i analyser at the British Antarctic Survey (BAS), with an accuracy of 0.3 and 0.9 ‰ respectively. The measurements are reported against the international standard of Vienna Standard Mean Ocean Water (V-SMOW). Deuterium excess (d_{ex}) is the second-order parameter calculated from the two water isotope ratios ($d_{\text{ex}} = \delta\text{D} - 8 \cdot \delta^{18}\text{O}$) (Dansgaard, 1964).

2.4. Major ion chemistry

Major ion concentrations were measured using a high-performance Dionex Integrion ion chromatograph with an injection volume of 250 μL in a class-100 cleanroom at BAS. For the cation chromatograph, we applied a guard column type CS16-4 μm (2×50 mm) and a CS16-4 μm separator column (2×250 mm). For the anion chromatograph, we used an AG17-C guard column (2×50 mm) together with an AS17-C analytical column (2×250 mm). The chemical data presented here is for the purposes of annual layer counting. Ions include sulphate [SO_4^{2-}], methanesulphonic acid [MSA], Bromide [Br^-] and Sodium [Na^+], with an analytical precision, defined as the relative standard deviation of the lowest level standard, of 0.03, 0.07, 0.003, and 0.07 ppb respectively.
120

2.5. Snow accumulation

125 The annual snow accumulation is derived from the annual layer thickness (see section 3.1). The thickness is converted to meters of water equivalent ($\text{m w}_{\text{eq}} \text{y}^{-1}$) based on the measured density. Thinning is corrected using the Nye model, which assumes thinning is proportional to vertical stress, appropriate for the upper 10% of the ice sheet. While the ice sheet thickness is unknown at this site, GPR confirms that bedrock is at least deeper than



43 m (Thomas et al., 2021). Given the sites elevation (730 m. a.s.l), and the relatively flat surface topography, a
 130 depth of 130 m (ensuring the firm core bottom depth was within the top 10% ice thickness) is not unreasonable.
 However, we acknowledge that this may not be the most appropriate thinning function for this site.

2.6. Estimating uncertainty

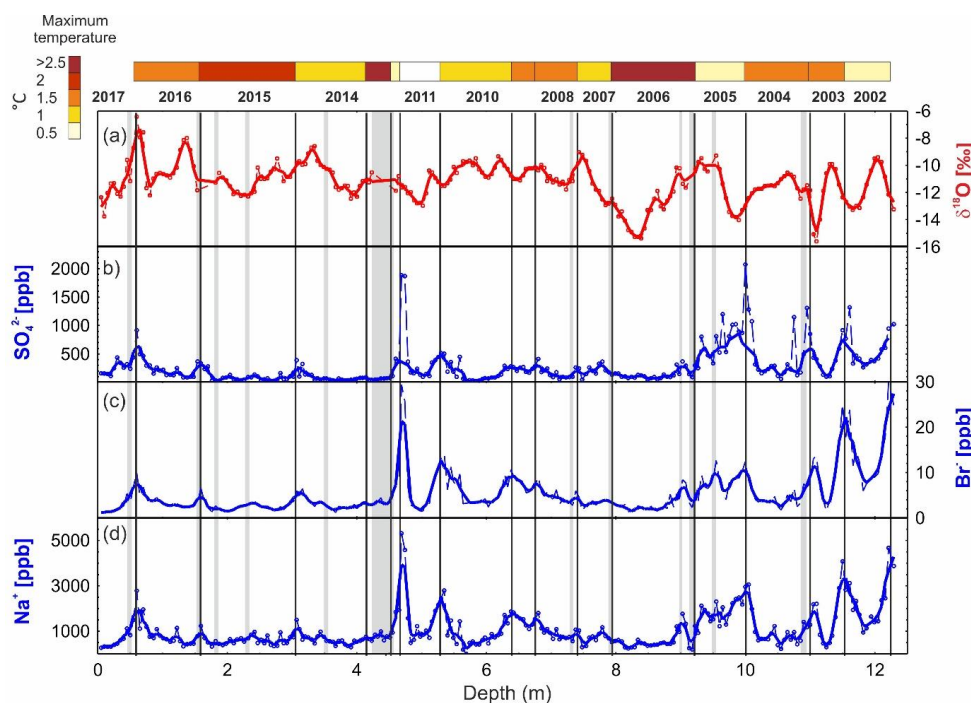
Uncertainty bars of 1 standard error (σ) are applied to all time series, except for 2006 (9.2 m) and 2013 (4.5 m)
 135 where a 2σ value is applied to account for the influence of melt (section 3.2). For the predicted bottom age
 estimate (section 4), the uncertainty estimate is calculated based on the difference between an upper and lower
 snow accumulation estimate. The lower value is based on the snow accumulation derived using all 15 years and
 the upper value derived with the two high melt years removed.

3. Results:

3.1. Age-scale

140 The age-scale has been derived using annual layer counting, based on the seasonal deposition of major ion
 chemistry (Fig. 2). Given its maritime location, seasonal cycles are especially clear in chemical species with
 marine origin, including $[\text{SO}_4^{2-}]$, $[\text{MSA}^-]$ and $[\text{Br}^-]$. These species relate to changes in marine productivity and
 sea ice (e.g., Thomas et al., 2019 and references therein), which peak during the phytoplankton bloom in spring
 and summer. Both $[\text{SO}_4^{2-}]$ and $[\text{MSA}^-]$ are robust seasonal markers in many coastal Antarctic ice cores
 145 (Emanuelsson et al., 2022; Tetzner et al., 2022; Thomas and Abram, 2016), and have also proved to be valuable
 for dating other sub-Antarctic ice cores (King et al., 2019; Moser et al., 2021).

Summer peaks were assigned if a consistent peak was observed in the marine ions (Fig. 2b-d). The stable water
 isotope record (Fig. 2a) was used as a secondary tracer. An equal number of peaks are identified in the isotope
 and ions records, however, there is often an offset in the location of the peak. For consistency, the location of
 150 the major ion peak was used. Thus, the age is assumed to represent approximately December – November
 corresponding to the summer sea ice break-up. The final age-scale extends from summer 2017 until summer
 2002, encompassing 15 full years.

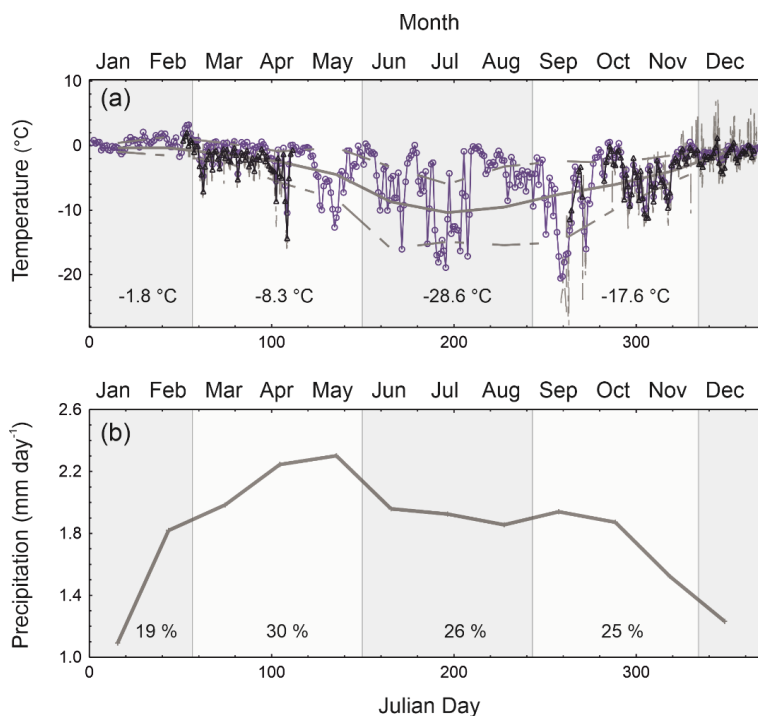




155 **Figure 2: Annual layer counting based on (a) Stable water isotopes ($\delta^{18}\text{O}$), (b) Sulphate (SO_4^{2-}), (c) Bromide (Br^-), and (d) Sodium (Na^+) all plotted at 5 cm resolution (dashed curves) with a 3-point running mean (solid curves). Vertical black lines indicate the location of summer peaks. Vertical grey shading indicates observed melt layers of greater than 5 cm thickness. Top colour bar represents the maximum daily 2m temperature from ERA5.**

160 **3.2. Evaluating the skill of ERA5 reanalysis to capture temperature**

The Peter 1st firn core and the in-situ observations from an AWS provides a unique opportunity to evaluate the skill of the latest generation of reanalysis, ERA5, at a remote Sub-Antarctic Island. The hourly temperature data recorded by the AWS has been converted to daily averages for comparison (Fig. 3a). The AWS recorded intermittently from February to December 2006, and averages were only calculated on days when greater than 50% of the hourly data was available. There is exceptional agreement between the AWS and ERA5 daily data, with a correlation coefficient of $r=0.91$ for the days of overlap ($n=149$, $p<0.0001$). This demonstrates the high degree of skill in the ERA5 reanalysis data, although the period of comparison is short. The average daily temperature from the AWS data was $-3.09\text{ }^\circ\text{C}$, $0.93\text{ }^\circ\text{C}$ colder than the same days in ERA5.



170 **Figure 3: Seasonal cycle in temperature (a) and precipitation (b) at Peter 1st island from ERA5 reanalysis (grey curve) (2002-2016 CE). Dashed grey curve represents 2.5 % and 97.5 % percentiles for temperature (a). Daily average temperatures during 2006 CE from ERA5 (blue circle) and AWS (black triangle), with hourly AWS temperature shown in thin grey curve. Grey shading highlights the seasons, with the corresponding average temperature and percentage of precipitation shown. AWS data available from University of Wisconsin-Madison Automatic Weather Station Program.**

The AWS was positioned at 128 m above sea level, while the ERA5 data is 2 m above sea level and the ice core was drilled at 730 m. To account for the adiabatic rate of temperature change for vertically moving air, a lapse rate is applied. The lapse rate varies dependent on the temperature and mixing ratio and is unknown for this site. A lapse rate of $0.68\text{ }^\circ\text{C}/100\text{ m}$ was applied in Thomas et al., (2021) for the SubICE sites, based on a rate estimate for the western AP (Martin and Peel, 1978), assumed to be representative of the maritime locations.



However closer evaluation of the in-situ AWS data, and the interpretation of melt features at Peter 1st, suggest this lapse rate may not be appropriate.

185 If the lapse rate of 0.68°C/100 m is applied the offset in average daily temperature between ERA5 (2 m) and the AWS (128 m) is just 0.07 °C. A recent evaluation of the bias between ERA5 and Antarctic temperatures suggested ERA5 has a warm bias of 0.58 °C for the AP and -0.66 °C for West Antarctica (Zhu et al., 2021). In addition, if the western AP lapse rate is applied to ERA5 this would suggest that daily mean site temperatures at the drill site never exceed -1.7 °C in the period 2002-2016. This does not fit with the evidence of visible melt features in the firn core.

190 If we assume that the multiple melt features at ~9.2 m depth correspond to the positive degree days during February 2006, then we would expect that site temperatures have exceeded 0 °C. Even if only for a few hours. The warmest daily average temperature from the AWS (February 2006) was 1.94°C. The appearance of melt features results from a dynamic interplay of atmospheric and snow conditions, but if melting generally occurs during positive temperatures, a minimum lapse rate of 0.32°C/100 m is required to allow for positive
195 temperatures at the drill site (602 m higher in elevation). This is lower than the moist adiabatic lapse rate (0.4-0.6 °C/100 m), and lower than lapse rates measured at the Sub-Antarctic Macquarie Island (Fitzgerald and Kirkpatrick, 2020). However, lapse rates as low as 0.31 °C/100 m have been reported at the Sub-Antarctic Marion Island (Nyakatyia and McGeoch, 2008).

200 3.3. The relationship between temperature and surface melt.

An evaluation of the visible melt layers for this site suggests that 11 % of the total ice core is classified as melt (Thomas et al., 2021). This percentage is driven largely by a single 30 cm thick melt layer at a depth of 4.5 m (Fig. A1). Based on our annual layer counting, constrained by the [SO₄²⁻] peak at 4.6 m, this melt feature corresponds to the year 2013 CE. Over a period of 21 days in January 2013, the daily temperature (ERA5, not
205 corrected for elevation) remained above 0.5°C, reaching a maximum daily temperature of 2.5 °C (Fig. 2). The prolonged mild conditions likely explain the thick melt feature.

The second meltiest year on the record is 2006 CE. A maximum daily temperature of 3.2°C (ERA5) was recorded in February 2006, the warmest month in the record. Between February and March 2006, maximum daily temperatures exceeded 0.5°C for a total of 39 days. Positive temperatures during 2006 are corroborated by
210 AWS data, which recorded a maximum daily temperature of 1.94 °C. The highest hourly temperature recorded by the AWS was 7.1 °C, in December 2006 (Fig. 3).

A positive relationship is observed between maximum daily 2 m temperatures and melt thickness ($r=0.4$, $p<0.1$). Once the total melt thickness in each year is converted to a melt percentage (dividing the total melt thickness by annual layer thickness), the correlation with 2 m maximum temperatures increases to $r=0.5$ ($p<0.1$). The broad
215 alignment of the melt layers alongside the peaks in chemical species, provide additional evidence for a summer peak. The evidence that the warmest years on the record, 2006 and 2013 CE, correspond to the most melt affected sections in the core provide independent verification for the proposed age-scale.

3.4. Evaluating the skill of ERA5 reanalysis to capture precipitation.

220 In the absence of daily precipitation data from the AWS, we can use the snow accumulation derived from the firn core to evaluate the skill of ERA5 in capturing inter-annual precipitation variability. The average snow accumulation derived from the firn core (2002 – 2016) is 0.49 m weq yr⁻¹. This is slightly lower than the estimated precipitation – evaporation (P-E) value of 0.55 m weq yr⁻¹ from ERA5 for this site (Fig. 4a). Case studies on the AP and coastal Ellsworth Land, using the previous generation of reanalysis products (ERA-Interim and ERA-40), suggest that snow accumulation is underestimated by between 0.025 and 0.26 m weq per
225 year (Thomas and Bracegirdle, 2009; Thomas and Bracegirdle, 2015). In this more maritime setting, and notwithstanding the different orographic positions of the firn core site on the island, there is an offset of approximately 6 cm per year (~12%) between the snow accumulation recorded in the firn core and ERA5 (P-E).

230 Snow accumulation is the sum of precipitation, evaporation, melt, erosion, and sublimation. Wind driven erosion and re-distribution is estimated to remove between 5-20 cm yr⁻¹ of precipitated snow in Antarctic



coastal regions (Lenaerts and van den Broeke, 2012). Within the lower range of our observed offset. In addition, we have already established that this site is influenced by melt, which not only alters the density calculations, but may also suggest potential loss as melt run-off. Removing all years where the percentage of the annual layer thickness classified as melt exceeds 20% (years 2006 and 2013 CE), the revised snow accumulation ($0.53 \text{ m weq yr}^{-1}$) is just 2 cm ($\sim 4\%$) lower than the ERA5 P-E.

3.5. Snow accumulation

Snow accumulation (2016 – 2002) at Peter 1st is positively correlated with P-E from ERA5. Strong correlations are observed over the island ($r=0.75$, $p<0.01$), with an extended zone of correlation ($r>0.6$) across the Bellingshausen Sea, the AP, and the Ronne-Filchner ice shelf (Fig. 4b). This relationship between snow accumulation at Peter 1st and the adjacent Ellsworth Land coast is confirmed by comparison with the snow accumulation record from the Ferrigno ice core drilled in 2010 (Thomas et al., 2015). Despite the short period of overlap ($n=9$), the two records are positively correlated ($r=0.62$, $p<0.1$) with a similar average snow accumulation rate ($0.55 \text{ m weq yr}^{-1}$ at Ferrigno).

A positive correlation is also observed between snow accumulation and surface air temperature from ERA5 ($r=0.58$, $p<0.05$). The spatial extent of the correlations (not shown) broadly mirrors the relationship with precipitation (Fig. 4b), extending from the Bellingshausen Sea over the AP.

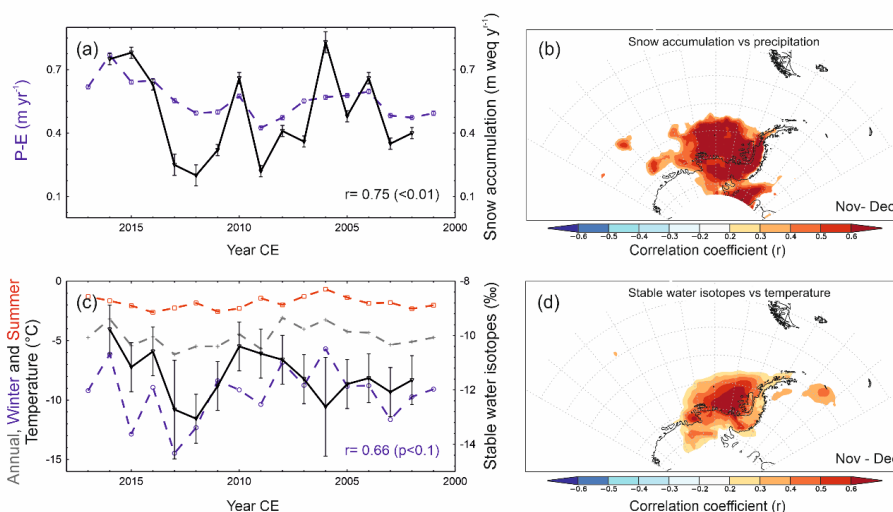


Figure 4: (a) Peter 1st annual average snow accumulation (solid black), compared with precipitation-evaporation (P-E) (dashed blue) from ERA5 reanalysis data (2001-2017) with corresponding correlation coefficients (r) value shown. (b) Spatial correlation plot of annual snow accumulation with annual ERA5 P-E (all coloured areas $p>0.05$). (c) Annual average stable water isotope ($\delta^{18}\text{O}$) (solid black), compared with 2 m temperatures from ERA5, as annual (grey dashed), summer (red dashed) and winter (blue dashed) averages. Correlation coefficient (r) between annual $\delta^{18}\text{O}$ and winter average 2m temperature after high melt years removed. (d) Spatial correlation plot of annual $\delta^{18}\text{O}$ with annual ERA5 2m temperature (all coloured areas $p.0.05$). All annual averages calculated as December to November, summer December to March and winter June-August. Uncertainty bars are one standard error (σ), for all years except 2006 and 2013, where 2σ are applied to account for additional uncertainties relating to melt.

3.6. Stable water isotopes

The stable water isotope composition of Antarctic snowfall has been used to reconstruct past surface temperatures at annual to centennial timescales (e.g., (Stenni et al., 2017) and reference therein). However, the processes controlling isotopic composition are complex, relating to water vapour origin, distance from source



(Hatvani et al., 2017), condensation conditions, fractionation pathways (Markle and Steig, 2022), precipitation seasonality, intermittency and post-depositional changes (Münch et al., 2017; Fernandoy et al., 2012).

265 The annual average stable water isotopes (both $\delta^{18}\text{O}$ and δD) at Peter 1st are weakly correlated with ERA5 2 m temperatures at the site ($r=0.37$, $p>0.1$) (Fig. 4c). Removing the two most melt affected years (2013 & 2006 CE) and comparing the annual record with winter average 2m temperature (June-August), increases the correlation with 2 m temperatures to $r=0.61$ ($p<0.05$) (Table 1) and $r=0.66$ ($p<0.05$) respectively.

270 The relationship between $\delta^{18}\text{O}$ and temperature is much stronger over the adjacent ocean (Fig. 4d). The spatial correlation plot reveals a strong positive correlation with 2 m temperature over the Bellingshausen Sea ($r>0.6$), within the approximate area of the seasonal sea ice zone.

3.7. Major ions

As expected for an island location, the major ions deposited at Peter 1st are largely of marine origin. The ratio of Cl^-/Na^+ in the ice core is 1.8, consistent with the standard seawater ratio (1.79). Thus, at this site $[\text{Na}^+]$ can be considered primarily of marine origin (~95%). The $\text{Cl}^-/\text{Mg}^{2+}$ and $\text{Cl}^-/\text{Ca}^{2+}$ ratios suggest that seawater accounts for 82% and 73% of the $[\text{Mg}^{2+}]$ and $[\text{Ca}^{2+}]$ concentration respectively.

280 The average $[\text{Na}^+]$ at Peter 1st is 998 ppb, consistent with a coastal location. A database of 105 Antarctic ice cores (Thomas et al., 2022) suggest that the highest $[\text{Na}^+]$ in an Antarctic ice core is observed on the Fimbul ice shelf, coastal East Antarctica, where average concentrations exceed 2700 ppb. The average $[\text{Na}^+]$ at Peter 1st is higher than the Sub-Antarctic Island of Bouvet, in the South Atlantic, where the average $[\text{Na}^+]$ was 101 ppb (King et al., 2019). It is also higher than values on the AP, which range between 50-215 ppb (Emanuelsson et al., 2022; Thomas et al., 2022), however, the drill sites are higher in elevation and further from the oceanic source.

285 The average $[\text{SO}_4^{2-}]$ at Peter 1st is 267 ppb. This is considerably higher than concentrations found in AP ice cores, where values of between ~30 and 70 ppb are observed (Thomas et al., 2022; Emanuelsson et al., 2022). However, higher concentrations are observed at Bouvet Island (King et al., 2019) (529 ppb) and the Fimbul ice shelf (536 ppb) (Thomas et al., 2022).

3.8. Source regions and transport pathways of snowfall

290 To establish the potential source regions of proxies, and their transport routes to the site, we evaluate the snow accumulation against climate parameters from ERA5 and common climate indices (Table 1). However, we acknowledge that the short duration of the ice core record may lead to spurious or not statistically significant results. Thus, we have generated a “pseudo core” based on the P-E extracted from ERA5 at the firn core location. Spatial correlations are run using the 15 years of firn core data, the same 15-year window (2002 – 2016) for the pseudo core and the extended 37 years (1979 – 2016) of pseudo core data (Fig. 5).

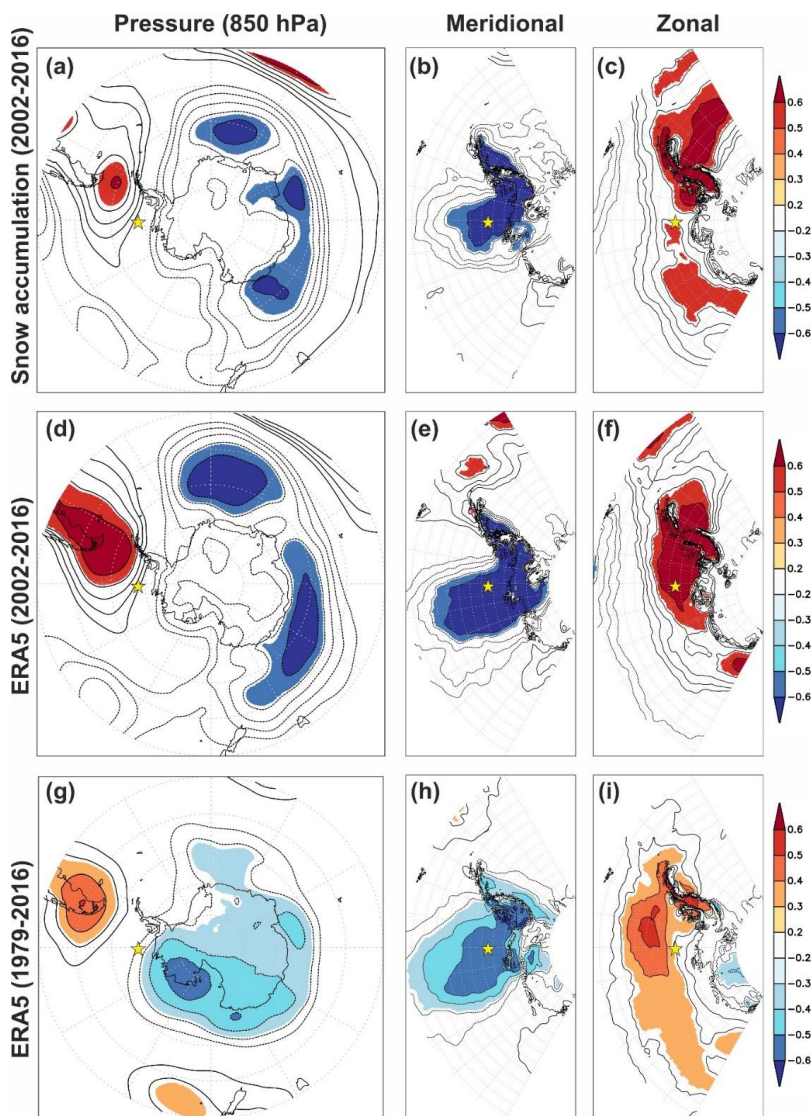
295 The spatial correlation between snow accumulation (P-E for the pseudo cores) and geopotential height (850 hPa) are shown in figures 5a, 5d and 5g. A distinct pattern of positive correlations is observed over the southern tip of South America and the Drake Passage, with opposing negative correlations over the Atlantic and Indian sectors of the Southern Ocean. The spatial correlations are remarkably similar when using both the firn core derived snow accumulation and the pseudo core data over the same period (Fig. 5d). Over the extended period (1979–2016) the positive correlation remains over southern South America, suggesting this feature is robust over the 37-year period (Fig. 5g). However, the region of negative correlations shifts from over the ocean to over the Antarctic continent, in a pattern reminiscent of the Southern Annular Mode (SAM) (Marshall, 2003).

300 Meridional winds draw warm-moist air from the South Pacific sector of the Southern Ocean as shown by the strong correlations between snow accumulation and meridional winds (blue area in Fig. 5b, 5e and 5h). The blocking high- and low-pressure anomalies to north and south of the AP funnel the air-masses from the Bellingshausen Sea, over the AP and into the Weddell Sea sector. This zonal transport is shown by the correlations between snow accumulation and westerly winds (red area in Fig. 5c, 5f, and 5i) across the AP. Thus, enhanced precipitation (more snow accumulation) is associated with stronger northerly and westerly winds across the Amundsen and Bellingshausen Seas. This spatial pattern in meridional winds is observed for the firn core period (2002-2016) and maintained over the longer period (1979-2016), suggesting a degree of stability over decadal timescales. However, there is a definite southward shift in the correlations with zonal

310



winds. During the shorter period of the firn core record, the strongest correlations are with winds at the same latitude or slightly south of the island. However, during the extended period (1979-2016) (Fig. 5i) the highest correlations are observed to the north of the island, further away from the coast of West Antarctica.



315

Figure 5. Exploring the mechanisms driving precipitation variability at Peter 1st Island (yellow star). Spatial correlation between Peter 1st snow accumulation and (a) geopotential height (850 hPa), (b) meridional winds and (c) zonal winds (ERA5, 2002-2016). Plots d-f are the same spatial correlations but using a timeseries of P-E extracted from ERA5 for the ice core site (“pseudo cores”). Plots g-i are the same but for the extended period 1979 – 2016.

320

The snow accumulation is positively correlated with the SAM ($r=0.59$, $p<0.05$), with a comparable correlation to that when using the pseudo core data (ERA5 P-E, $r=0.55$, $p<0.05$). The correlation with SAM becomes weaker when using the extended pseudo record (1979 – 2016), $r=0.3$ ($p<0.1$). Snow accumulation is negatively



325 correlated with the Southern Oscillation Index (SOI), $r = -0.48$ ($p < 0.1$). The SOI is the normalized pressure
 difference between Tahiti and Darwin, which tracks the atmospheric component of El Niño Southern Oscillation
 (ENSO). This suggests that snowfall on the island (and potentially the proxies contained therein) is influenced
 by large-scale modes of atmospheric variability and tropical teleconnections. However, the correlation between
 the pseudo core (P-E) and SOI is not significant ($p > 0.1$) over the 15-year period of the firn core (2002-2016), or
 330 the extended period (1979-2016). This suggests that the relationship with both climate indices is not temporally
 stable as observed in other studies (e.g., Thomas et al., 2015). We do not find any correlation between $\delta^{18}\text{O}$ with
 either SOI or SAM. The correlation is not improved by removing the highest melt years (2013 & 2006). There is
 also no correlation between 2 m temperature (ERA5) with either SOI or SAM, suggesting that temperatures at
 the site are not influenced by large-scale modes of variability, at least over short timescales.

335 **Table 1: Comparing the annual average 2 m temperature (2 m Temp) and P-E data from ERA5 with the
 annual average stable water isotopes ($\delta^{18}\text{O}$) and snow accumulation data from the Peter 1st firn core. The
 2 m Temp range at the firn core location (730 m a.s.l) is calculated based on a lower lapse rate of $0.31\text{ }^\circ\text{C}/$
**100 m and an upper lapse rate of $0.68\text{ }^\circ\text{C}/100\text{ m}$ (Thomas et al., 2021). Correlation coefficient between
 SAM, SOI, P-E and 2m temperature are shown only if $p < 0.05$ ($n=15$). The correlations when the two
 340 melt years (2006 & 2013) are removed are shown in brackets ($n=13$).****

Species	Mean	Max	Min	SAM (r)	SOI (r)	ERA5 (P-E) (r)	ERA 2m Temp (r)
ERA5							
2m Temp ($^\circ\text{C}$) (Sea level)	-4.6	-3.0	-6.2			0.60	
2 m Temp ($^\circ\text{C}$) (730 m a.s.l)	-9.4 to -6.8	-7.8 to -5.3	-11.0 to -8.4			0.60	
P-E (m weq)	0.55	0.77	0.43	0.55			0.60
Peter 1st firn Core							
$\delta^{18}\text{O}$ (‰)	-11.3‰	-6.4 ‰	-15.6 ‰				(0.61)
Snow accumulation m weq	0.49 (0.53)	0.83 (0.77)	0.20 (0.22)	0.59	-0.48	0.75 (0.85)	0.58

4. Discussion:

The objective of this study is to establish if a firn core from Peter 1st Island is suitable for paleoclimate
 reconstructions. Here we discuss the climatological data captured by the firn core and explore this sites potential
 345 for future deep ice core drilling.

4.1. Annual layer counted age-scale.

We have established that seasonal cycles in major ion chemistry and $\delta^{18}\text{O}$ are suitable for annual layer counting.
 A prominent peak in major ion chemistry (including $[\text{SO}_4^{2-}]$) at 4.6 m depth corresponds to the Puyehue-Cordon
 Caulle eruption from southern Chile. This VEI5 rated eruption began in June 2011 and appears in our record
 350 from late 2011 and into 2012 and provides at least one independent reference horizon. High biogenic $[\text{SO}_4^{2-}]$
 background can make identification of volcanic $[\text{SO}_4^{2-}]$ peaks difficult, as demonstrated at Antarctic Peninsula
 sites (Emanuelsson et al., 2022; Tetzner et al., 2021). While the average $[\text{SO}_4^{2-}]$ is lower at Peter 1st than many
 coastal Antarctic sites, the background $[\text{SO}_4^{2-}]$ may make identification of bi-polar eruptions difficult, and the
 presence of volcanic ash (tephra) may be required to identify volcanic tie points in a deeper ice core from this
 355 site. The lower end of the age-scale is constrained by the absence of the recently identified Sturge island
 eruption in 2001 (Tetzner et al., 2021). This Sub-Antarctic eruption has been detected as large shards in other
 Sub-Antarctic islands (Moser et al., 2021) and the Ellsworth Land coast adjacent to Peter 1st. Although not
 definitive, if our age-scale extended beyond 2002, we might expect to see some evidence of this eruption at this
 site.



360 The bottom age of 2002 CE is within the uncertainty range of a previous estimate (2004 +/- 2 years), based on
the fitted density profile using the P-E from ERA5 (Thomas et al., 2021). When using the newly calculated
snow accumulation (0.49 m weq yr⁻¹), the updated density derived bottom age is 2002 +/- 1 years. Thus,
validating the use of the densification model to estimate the potential bottom age for a deeper ice core. The
density profile estimate suggests that an ice core drilled to the maximum GPR layer depth (identified at 43 m
365 (Thomas et al., 2021)), would provide a record dating back to 1951.2 CE +/- 5 years. While the ice sheet
thickness remains unknown, based on the measured snow accumulation rate and density profile, we conclude
that an ice core drilled to 100 m depth would provide a record dating back to 1833 CE +/- 13 years.

4.2. Proxy validation and comparison with reanalysis (ERA5)

370 With only a single AWS temperature record, that does not comprise a full year and is some distance from the ice
core site, we must rely on the reanalysis data to evaluate our proxy measurements. The previous ECMWF
reanalyses products (ERA-Interim and ERA-40) have been tested widely in Antarctica (e.g., (Bromwich and
Fogt, 2004)) and at sites in the adjacent Ellsworth Land coast and the AP (Thomas and Bracegirdle, 2009;
2015). A recent study confirms that ERA5 accurately captures variability across Antarctica (Zhu et al., 2021)
and in near-surface air temperature and wind regimes over the adjacent AP (Tetzner et al., 2019).

375 The high correlation between daily mean 2 m temperature in ERA5 and temperature recorded in an AWS
demonstrate the high degree of skill in ERA5 at this location. The correlation of 0.91 is consistent with the
correlation of 0.92 determined when comparing observations and ERA5 annual mean temperatures for
Antarctica (Zhu et al., 2021). However, in the absence of a measured lapse rate it is difficult to determine the
true temperature bias in the ERA5 reanalysis for Peter 1st. If we apply the lapse rate of 0.32 °C/100 m (proposed
380 in section 3.2) this suggests that ERA5 has a cold bias of 0.37°C.

Comparing the 15 years of annual mean snow accumulation from the firm core with P-E from ERA5 (Fig. 4a)
revealed a high temporal correlation between the two records ($r = 0.75$, $p < 0.01$; Table 1) and comparable
absolute values. The slight over-estimation of the ERA5 total P-E (~ 4-6 %) is less than the offset observed at
adjacent sites on the AP (Thomas and Bracegirdle, 2009:2015). The slight offset is likely an artefact of the
385 resolution of the ERA5 reanalysis data (0.25° resolution (~ 31 km)), which is not sufficient to differentiate Peter
1st island from the surrounding ocean. However, despite this limitation our study suggests that ERA5 displays a
high degree of skill in capturing absolute amount and temporal variability in precipitation changes, at this firm
core site on a small and mountainous island location. Importantly, the spatial correlation maps reveal that the
high correlation between snow accumulation and ERA5 P-E extends over the AP and Amundsen-
390 Bellingshausen Sea region (Fig 4b). These results support the use of the firm core for regional climate
reconstructions.

4.3. Relationship between snow accumulation and stable isotopes with precipitation and temperature

The strong correlation ($r=0.75$, $p<0.01$; Table 1) between annual snow accumulation and P-E in the
corresponding ERA5 grid cell over the common 15-year interval suggests that the ice core layer thickness (snow
395 accumulation) is dominated by changes in precipitation. Thus, a longer reconstruction could provide valuable
insight into changes in snow accumulation and surface mass balance across a large and dynamic region of
Antarctica. Although traditionally viewed as a proxy for past surface temperature, the annual average $\delta^{18}\text{O}$ at
this site is not correlated with site annual average ERA5 2 m temperature (0.37, $p=0.17$). However, the observed
weak correlation coefficients ($\delta^{18}\text{O}$ vs 2m surface air temperature) are consistent with ice cores from the AP and
400 coastal Ellsworth Land (e.g., Thomas et al., 2009; 2013). The correlation between $\delta^{18}\text{O}$ and temperature is
improved by removing the melt years and correlated with winter average 2m temperatures. This may suggest
that winter conditions play a more dominant role in modulating $\delta^{18}\text{O}$ at this site, or that the summer $\delta^{18}\text{O}$ signal
is weaker or been lost. The summer months (December – February) receive the lowest amount of snowfall (Fig
3b), just 19% of the total. Thus, the isotopic signal (which is precipitation biased) will be more strongly
405 weighted to the spring, winter, and autumn months respectively. In addition, the summer months may
experience more melting, potentially smoothing the isotopic signal of the summer snow deposits.

At Peter 1st, the annual snow accumulation is strongly related to annual ERA5 2m surface air temperatures. The
positive correlation between snow accumulation and ERA5 2m T ($r=0.61$, $p<0.01$) reflects the relationship
between temperature and the saturation water vapour pressure governed by the Clausius–Clapeyron relation.
410 This relationship has been observed at ice core sites across the AP (e.g., Thomas et al., 2017), confirmed at the



continental scale (Medley and Thomas., 2019) and in a data-assimilation approach using global circulation models (Dalaiden et al., 2021). In the correlation map (Fig. 4d), there is a significant region of correlation between $\delta^{18}\text{O}$ and 2 m temperatures over adjacent ocean, especially within the seasonal sea ice zone. This suggests that sea ice may play a role in modulating $\delta^{18}\text{O}$ at this site. Sea ice has been shown to directly alter $\delta^{18}\text{O}$, through an enrichment of the water vapour (Bromwich and Weaver, 1983). A reduction in the length of the sea ice season and an overall decline in sea ice coverage in the Amundsen and Bellingshausen Seas has been attributed to the warming trends observed in previous West Antarctic reconstructions (Küttel et al., 2012; Steig et al., 2009; Thomas et al., 2013). Thus, we conclude that over longer timescales $\delta^{18}\text{O}$ and snow accumulation from any future ice cores from this site will capture changes in surface air temperatures in this region.

4.4. Drivers of variability and the influence of atmospheric modes

The record is too short to draw robust conclusions about the role of large-scale atmospheric circulation. However, given the islands location we expect this site to be strongly influenced by the Amundsen Sea Low (ASL), a climatological low-pressure system that exerts considerable influence on the climate of West Antarctica (Hosking et al., 2013). Enhanced northerly flow over the Bellingshausen Sea during the positive phase of the SAM has been attributed to the large increase in snowfall during the late 20th century (e.g., Thomas et al., 2017; Medley and Thomas, 2019). The observed relationship between annual snow accumulation at Peter 1st and annual meridional winds over the Bellingshausen Sea replicates the pattern seen at several AP sites (Thomas et al., 2008; 2015; 2017). This shared transport route is confirmed in the back trajectory analysis from the AP sites, which are dominated by air masses that cross directly over Peter 1st Island (Thomas and Bracegirdle, 2015).

Pressure in the ASL region is strongly modulated by large-scale modes of variability, especially SAM and ENSO (Fogt et al., 2012; Hosking et al., 2013). Despite the short period investigated, the snow accumulation does display significant relationships with both SAM (positive) and ENSO (negative). However, we are unable to ascertain the stability of this relationship, which has been proven to vary temporally at many sites across West Antarctica (Thomas et al., 2015; Wang et al., 2017). Indeed, the spatial correlation of annual average P-E from the Peter 1st site (ERA5 “pseudo core”) displays a stronger and more distinct spatial SAM pattern when using the longer record (Fig. 5g) than the period from 2002-2016 captured by the firn core. However, the correlation between annual SAM and annual average P-E in the 37-year pseudo core is lower than the 15-year period captured by the firn core, $r=0.30$ and $r=0.55$ (Table 1) respectively. This likely reflects the non-stationarity of the correlations between SAM and snow accumulation. Since the late 1990s, and the period captured by the firn core, the SAM has been predominantly in its positive phase, while the period from 1979-2016 is characterised by a shift from negative to positive SAM phase (Marshall, 2003).

While we might expect the ASL to influence the snow accumulation at Peter 1st, the relationship with snow accumulation and geopotential height in this region is not particularly strong. Instead, the Peter 1st annual snow accumulation (and the pseudo core data) appears more strongly influenced by the high-pressure anomalies over the Drake Passage, to the north of the AP. Long-lived, and relatively stationary anticyclones have been shown to influence snow accumulation over West Antarctica (Emanuelsson et al., 2018) by impeding the westerly circulation. These anticyclones, also known as blocking events, can deflect marine air towards to continent, resulting in increased precipitation. This may also reflect a shift in circulation patterns, as the observed trend toward deeper sea level pressures over the ASL region during the late 20th century has become less pronounced during the early 21st century. Indeed, this shift in circulation patterns has, in part, been attributed to the slowdown in the warming trend observed in the AP (Turner et al., 2016). Therefore, over longer time periods we might expect that snow accumulation from a future deep ice core would capture changes in ASL and blocking event variability.

4.5. Drivers of surface melt and the impact on proxy preservation

Despite its maritime location, Peter 1st island is situated south of the polar front at a comparable latitude to much of the East Antarctic coastline (~70°S). While the annual average temperature (1979-2017) is -9.5 °C, with summer temperatures of -5.1 °C (Thomas et al., 2021), the daily temperatures from ERA5 indicate maximum temperature at the site has exceeded 3°C. This maximum in February 2006 was verified by in-situ observations from an AWS. Over the 15-year period (~5500 days) covered by the firn core, there were a total of 189 positive degree days. Many, but not all, of these positive degree days correspond to visible melt layers in the ice core. However, there are some notable exceptions where melt features do not coincide with positive degree days.



Many of the major melt periods also coincide with documented evidence of atmospheric rivers (ARs). These narrow bands of enhanced water vapour transport heat and moisture from the mid- to the high-latitudes and have been attributed to melt events across West Antarctica (Nicolas et al., 2017). Wille et al (2019) derived an AR detection algorithm to demonstrate that between 40-80% of surface melt on the western AP (1979-2017) is attributed to ARs that make landfall during the winter months (March-October). Many of the ARs identified in that study pass directly over Peter 1st Island and may explain the occurrence of visible melt features in the Peter 1st firn core during the winter months. The yearly percentage of AR occurrences calculated in Wille et al (2019) reveal that two of the most abundant AR years, 2006 and 2013, correspond with the strongest melt features in the firn core. The year 2010 also contained a high number of AR occurrences, however, this year does not correspond to any major melt features in our record. However, 2010 was a high snow accumulation year and the enhanced moisture transport characterised by ARs is also known to increase precipitation. The physical mechanisms relating ARs to surface melt are complex, and thus it may be possible that some ARs passing over Peter 1st result in increased precipitation, but not visible melt features. Or that the ARs during 2010 that made landfall in West Antarctica did not pass directly over Peter 1st island.

It is only during the most extreme years that melt has had a notable impact on the proxy preservation. A high-resolution evaluation of the melt features, and their impact on chemical elution, is subject to further study. However, there is some evidence that the chemical and isotopic records during the extreme melt event in 2013 have been altered. This is observed in the near homogeneous concentrations of major ion and $\delta^{18}\text{O}$ values during this melt feature, which appear to have removed the seasonal signal. The occurrence of melt has also likely increased the uncertainty in the snow accumulation calculations. For example, stronger correlations between snow accumulation (and $\delta^{18}\text{O}$) and precipitation (and temperature) are achieved when the two highest melt years (2013 and 2006) are excluded.

Instrumental records from the AP suggest that annual surface air temperatures have increased by approximately 2.5°C since the 1950s (Turner et al., 2005), with reports of record-breaking heatwaves in recent years (González-Herrero et al., 2022). This is corroborated by ice core records across the AP and coastal Ellsworth Land, which suggest a prominent warming trend during the latter half of the 20th century (Thomas et al., 2013; Thomas et al., 2009; Thomas. and Tetzner., 2018). Despite the absence of a significant warming trend during the 21st century (Turner et al., 2016), the temperatures during the 21st century are still considerably warmer than the early and mid-20th century. Thus, we might expect that the melt frequency observed during this period (2002-2016) will also be much higher than at any time in the recent past. A deeper ice core drilled from this location may be subject to melting in the surface layers, due to continued regional warming (González-Herrero et al., 2022), although the impact of melting is likely limited to the mid-20th century onwards.

This hypothesis is supported by the melt history obtained from the James Ross Island (JRI) ice core, in the north-eastern tip of the AP (Abram et al., 2013). Mean annual temperature of -14.31°C were reported at the JRI site during the 1980s (Aristarain et al., 1987) however, during the period 2001-2017 the annual average temperature increased to -7.5°C , warmer than the -9.5°C observed at Peter 1st. This may explain why the average melt layer thickness of 3.2 cm per year at JRI is higher than the observed 1.8 cm per year at Peter 1st.

The visible melt features at JRI display a clear acceleration in frequency during the late 20th century (Abram et al., 2013). However, this melt has not had a notable influence on the proxy preservation or subsequent paleoclimate reconstructions generated from this site (e.g., Abram et al., 2013).

5. Conclusions:

Here we present the first climatic interpretation of $\delta^{18}\text{O}$, and snow accumulation data contained in a firn core drilled on the remote sub-Antarctic Island of Peter 1st. We conclude that a deep ice core from this site has the potential to provide valuable paleoclimate reconstructions, exploring the ice-atmosphere-ocean interactions in the Bellingshausen Sea based on the following findings:

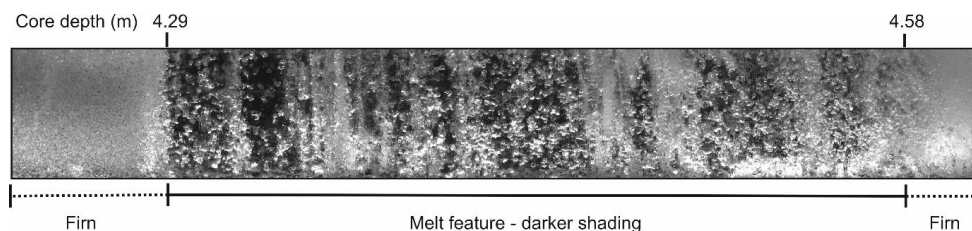
- The firn core can be annually layer counted and verified using a volcanic reference horizon from the Cordón Caulle eruption in 2011.
- The ERA5 reanalysis displays a high degree of skill at reproducing site surface temperature and snow accumulation. This is confirmed by comparing daily temperatures from an AWS against ERA5 2-m temperatures and by comparing annual average snow accumulation from the ice core against annual average precipitation (P-E) from ERA5 at the corresponding grid cell. Thus, demonstrating that ERA5 can capture



- 515 climate variability even at a small sub-Antarctic Island and supporting the use of ERA5 as a suitable dataset to interpret climate proxies in this firn core.
- Snow accumulation observed in the firn core is significantly correlated to both regional precipitation (P-E) changes and changes in surface air temperature.
 - Snow accumulation at the firn core site is likely related to large-scale modes of atmospheric variability, including SAM. However, the stability of the relationship between SAM and snow accumulation cannot be confirmed beyond the 15-year interval of the firn core.
 - 520 • The $\delta^{18}\text{O}$ record, although weakly correlated with site temperature, displays a strong and significant relationship with air temperature over the seasonal sea ice zone in the Bellingshausen Sea.
 - The melt frequency is lower than observed at existing deep ice core sites from coastal Antarctica. The melt features broadly correspond to temperature, with the two most extreme melt years (2006 and 2013) coincident with high temperatures and the documented occurrence of atmospheric rivers.
 - 525 • The GPR data from this site reveal near continuous stratified layers in the upper 43 m (Thomas et al., 2021).
 - While the ice sheet thickness remains unknown, based on the measured snow accumulation rate and density profile we conclude that an ice core drilled to 100 m depth would capture climate variability of the past ~200-years.

530

Appendices:



535 **Figure A1: Line scanned image of the Peter 1st firn core. Highlighting the prominent melt feature, observed as a dark area (higher density) between 4.29-4.58 m depth, compared to the lighter shaded (lower density) areas corresponding to firn.**

Data availability:

All data is submitted to the UK polar data centre (DOI pending) or available on request (lith@bas.ac.uk).

540

Author contributions:

ET designed the project and prepared the manuscript with contributions from all authors. JP, BM, GG conducted the fieldwork, DT produced the age-scale, DM contributed to the sample preparation, SJ conducted the IC analysis.

545 Competing interest:

ET is an editor of Climate of the Past. The peer-review process was guided by an independent editor, and the authors have also no other competing interests to declare."

Acknowledgements:

550 Funding was provided to subICE by École Polytechnique Fédérale de Lausanne, the Swiss Polar Institute, and Ferring Pharmaceuticals Inc. ERT received core funding from the Natural Environment Research Council to the British Antarctic Survey's Ice Dynamics and Palaeoclimate programme. Joel B. Pedro acknowledges support



from the European Research Council under the European Community's Seventh Framework Programme (FP7/2007e2013) and ERC grant agreement 610055 as part of the ice2ice project and from the Australian Government Department of Industry Science Energy and Resources, grant ASCI000002. We are grateful to the Norwegian Polar Institute for granting us permission to visit Peter Ist island. The authors appreciate the support of the University of Wisconsin-Madison Automatic Weather Station Program for the data set, data display, and information, NSF grant number 1924730 and ECMWF for providing ERA5 reanalysis data. We thank Laura Gerish (BAS) for producing the maps. We thank Joe Brown and Daniel Emanuelsson for the line scanning image presented in A1. Data used in this study are available through the UK Polar Data Centre. The authors would like to acknowledge the coordinators and participants of the Antarctic Circumnavigation Expedition for facilitating collection of the subICE cores, especially David Walton, Christian de Marliave, Julia Schmale, Robert Brett, Sergio Rodrigues, Francois Bernard, Amy King, Roger Stilwell, and Frederick Paulsen.

References:

- Abram NJ, Mulvaney R, Wolff EW, et al. (2013) Acceleration of snow melt in an Antarctic Peninsula ice core during the twentieth century. *Nature Geoscience* 6(5): 404-411.
- Abram NJ, Thomas ER, McConnell JR, et al. (2010) Ice core evidence for a 20th century decline in sea ice in the Bellingshausen Sea, Antarctica. *Journal of Geophysical Research* 115(D23).
- Aristarain AJ, Pinglot JF and Pourchet M (1987) Accumulation and Temperature Measurements on the James Ross Island Ice Cap, Antarctic Peninsula, Antarctica. *Journal of Glaciology* 33(115): 357-362.
- Bromwich DH and Fogt RL (2004) Strong Trends in the Skill of the ERA-40 and NCEP-NCAR Reanalyses in the High and Midlatitudes of the Southern Hemisphere, 1958–2001. *Journal of Climate* 17(23): 4603-4619.
- Bromwich DH and Weaver CJ (1983) Latitudinal displacement from main moisture source controls $\delta^{18}O$ of snow in coastal Antarctica. *Nature* 301(5896): 145-147.
- Dalaiden Q, Goosse H, Rezsöhazy J, et al. (2021) Reconstructing atmospheric circulation and sea-ice extent in the West Antarctic over the past 200 years using data assimilation. *Climate Dynamics*. DOI: 10.1007/s00382-021-05879-6.
- de Rosnay P (2018) T. Haiden, M. Dahoui, B. Ingleby, P. de Rosnay, C. Prates, E. Kuscü, T. Hewson, L. Isaksen, D. Richardson, H. Zuo, L. Jones.
- Emanuelsson BD, Bertler NAN, Neff PD, et al. (2018) The role of Amundsen–Bellingshausen Sea anticyclonic circulation in forcing marine air intrusions into West Antarctica. *Climate Dynamics* 51(9): 3579-3596.
- Emanuelsson BD, Thomas ER, Tetzner DR, et al. (2022) Ice Core Chronologies from the Antarctic Peninsula: The Palmer, Jurassic, and Rendezvous Age-Scales. *Geosciences* 12(2): 87.
- Fernandoy F, Meyer H and Tonelli M (2012) Stable water isotopes of precipitation and firn cores from the northern Antarctic Peninsula region as a proxy for climate reconstruction. *The Cryosphere* 6(2): 313-330.
- Fitzgerald NB and Kirkpatrick JB (2020) Air temperature lapse rates and cloud cover in a hyper-oceanic climate. *Antarctic Science* 32(6): 440-453.
- Fogt RL, Jones JM and Renwick J (2012) Seasonal zonal asymmetries in the Southern Annular Mode and their impact on regional temperature anomalies. *Journal of Climate* 25(18): 6253-6270.
- González-Herrero S, Barriopedro D, Trigo RM, et al. (2022) Climate warming amplified the 2020 record-breaking heatwave in the Antarctic Peninsula. *Communications Earth & Environment* 3(1): 122.
- Goodwin BP, Mosley-Thompson E, Wilson AB, et al. (2016) Accumulation Variability in the Antarctic Peninsula: The Role of Large-Scale Atmospheric Oscillations and Their Interactions. *Journal of Climate* 29(7): 2579-2596.
- Hatvani IG, Leuenberger M, Kohán B, et al. (2017) Geostatistical analysis and isoscape of ice core derived water stable isotope records in an Antarctic macro region. *Polar science* 13: 23-32.
- Hosking JS, Orr A, Marshall GJ, et al. (2013) The Influence of the Amundsen–Bellingshausen Seas Low on the Climate of West Antarctica and Its Representation in Coupled Climate Model Simulations. *Journal of Climate* 26(17): 6633-6648.
- Jenkins A and Jacobs S (2008) Circulation and melting beneath George VI Ice Shelf, Antarctica. *Journal of Geophysical Research: Oceans* 113(C4).
- King ACF, Thomas ER, Pedro JB, et al. (2019) Organic Compounds in a Sub-Antarctic Ice Core: A Potential Suite of Sea Ice Markers. *Geophysical Research Letters* 46(16): 9930-9939.
- Küttel M, Steig EJ, Ding Q, et al. (2012) Seasonal climate information preserved in West Antarctic ice core water isotopes: relationships to temperature, large-scale circulation, and sea ice. *Climate Dynamics* 39(7): 1841-1857.



- Lenaerts JTM and van den Broeke MR (2012) Modeling drifting snow in Antarctica with a regional climate model: 2. Results. *Journal of Geophysical Research: Atmospheres* 117(D5).
- 610 Li C, Michel C, Seland Graff L, et al. (2018) Midlatitude atmospheric circulation responses under 1.5 and 2.0 C warming and implications for regional impacts. *Earth System Dynamics* 9(2): 359-382.
- Markle BR and Steig EJ (2022) Improving temperature reconstructions from ice-core water-isotope records. *Clim. Past* 18(6): 1321-1368.
- 615 Marshall GJ (2003) Trends in the Southern Annular Mode from Observations and Reanalyses. *Journal of Climate* 16(24): 4134-4143.
- Martin PJ and Peel DA (1978) The Spatial Distribution of 10 m Temperatures in the Antarctic Peninsula. *Journal of Glaciology* 20(83): 311-317.
- Medley B and Thomas ER (2019) Increased snowfall over the Antarctic Ice Sheet mitigated twentieth-century sea-level rise. *Nature Climate Change* 9(1): 34-39.
- 620 Moser DE, Jackson S, Kjær HA, et al. (2021) An Age Scale for the First Shallow (Sub-)Antarctic Ice Core from Young Island, Northwest Ross Sea. *Geosciences* 11(9): 368.
- Münch T, Kipfstuhl S, Freitag J, et al. (2017) Constraints on post-depositional isotope modifications in East Antarctic firm from analysing temporal changes of isotope profiles. *The Cryosphere* 11(5): 2175-2188.
- 625 Nicolas JP, Vogelmann AM, Scott RC, et al. (2017) January 2016 extensive summer melt in West Antarctica favoured by strong El Niño. *Nature Communications* 8(1): 15799.
- Nyakatya M and McGeoch MA (2008) Temperature variation across Marion Island associated with a keystone plant species (Azorella selago Hook.(Apiaceae)). *Polar Biology* 31(2): 139-151.
- Paolo FS, Fricker HA and Padman L (2015) Volume loss from Antarctic ice shelves is accelerating. *Science* 348(6232): 327-331.
- 630 Parkinson CL (2019) A 40-y record reveals gradual Antarctic sea ice increases followed by decreases at rates far exceeding the rates seen in the Arctic. *Proceedings of the National Academy of Sciences* 116(29): 14414-14423.
- Porter SE, Parkinson CL and Mosley-Thompson E (2016) Bellingshausen Sea ice extent recorded in an Antarctic Peninsula ice core. *Journal of Geophysical Research: Atmospheres* 121(23): 13,886-813,900.
- 635 Pritchard HD, Arthern RJ, Vaughan DG, et al. (2009) Extensive dynamic thinning on the margins of the Greenland and Antarctic ice sheets. *Nature* 461(7266): 971-975.
- Ropelewski CF and Jones PD (1987) An Extension of the Tahiti–Darwin Southern Oscillation Index. *Monthly Weather Review* 115(9): 2161-2165.
- 640 Royles J, Amesbury Matthew J, Convey P, et al. (2013) Plants and Soil Microbes Respond to Recent Warming on the Antarctic Peninsula. *Current Biology* 23(17): 1702-1706.
- Siegert M, Atkinson A, Banwell A, et al. (2019) The Antarctic Peninsula Under a 1.5°C Global Warming Scenario. *Frontiers in Environmental Science* 7.
- Smith B, Fricker HA, Gardner AS, et al. (2020) Pervasive ice sheet mass loss reflects competing ocean and atmosphere processes. *Science* 368(6496): 1239-1242.
- 645 Steig EJ, Schneider DP, Rutherford SD, et al. (2009) Warming of the Antarctic ice-sheet surface since the 1957 International Geophysical Year. *Nature* 457(7228): 459-462.
- Stenni B, Curran MAJ, Abram NJ, et al. (2017) Antarctic climate variability on regional and continental scales over the last 2000 years. *Clim. Past* 13(11): 1609-1634.
- 650 Tetzner D, Thomas E and Allen C (2019) A Validation of ERA5 Reanalysis Data in the Southern Antarctic Peninsula—Ellsworth Land Region, and Its Implications for Ice Core Studies. *Geosciences* 9(7): 289.
- Tetzner DR, Allen CS and Thomas ER (2022) Regional variability of diatoms in ice cores from the Antarctic Peninsula and Ellsworth Land, Antarctica. *The Cryosphere* 16(3): 779-798.
- Tetzner DR, Thomas ER, Allen CS, et al. (2021) Evidence of Recent Active Volcanism in the Balleny Islands (Antarctica) From Ice Core Records. *Journal of Geophysical Research: Atmospheres* 126(23): e2021JD035095.
- 655 Thomas ER and Abram NJ (2016) Ice core reconstruction of sea ice change in the Amundsen-Ross Seas since 1702 A.D. *Geophysical Research Letters* 43(10): 5309-5317.
- Thomas ER, Allen CS, Etourneau J, et al. (2019) Antarctic Sea Ice Proxies from Marine and Ice Core Archives Suitable for Reconstructing Sea Ice over the Past 2000 Years. *Geosciences* 9(12): 506.
- 660 Thomas ER and Bracegirdle TJ (2009) Improving ice core interpretation using in situ and reanalysis data. *Journal of Geophysical Research: Atmospheres* 114(D20).
- Thomas ER and Bracegirdle TJ (2015) Precipitation pathways for five new ice core sites in Ellsworth Land, West Antarctica. *Climate Dynamics*. DOI: 10.1007/s00382-014-2213-6.
- 665 Thomas ER, Bracegirdle TJ, Turner J, et al. (2013) A 308 year record of climate variability in West Antarctica. *Geophysical Research Letters* 40(20): 5492-5496.
- Thomas ER, Dennis PF, Bracegirdle TJ, et al. (2009) Ice core evidence for significant 100-year regional warming on the Antarctic Peninsula. *Geophysical Research Letters* 36(20).



- 670 Thomas ER, Gacitúa G, Pedro JB, et al. (2021) Physical properties of shallow ice cores from Antarctic and sub-Antarctic islands. *The Cryosphere* 15(2): 1173-1186.
- Thomas ER, Hosking JS, Tuckwell RR, et al. (2015) Twentieth century increase in snowfall in coastal West Antarctica. *Geophysical Research Letters* 42(21): 9387-9393.
- Thomas ER, Marshall GJ and McConnell JR (2008) A doubling in snow accumulation in the western Antarctic Peninsula since 1850. *Geophysical Research Letters* 35(1).
- 675 Thomas ER, van Wessem JM, Roberts J, et al. (2017) Regional Antarctic snow accumulation over the past 1000 years. *Clim. Past* 13(11): 1491-1513.
- Thomas ER, Vladimirova DO, Tetzner DR, et al. (2022) Ice core chemistry database: an Antarctic compilation of sodium and sulphate records spanning the past 2000 years. *Earth Syst. Sci. Data Discuss.* 2022: 1-20.
- 680 Thomas. E, R and Tetzner. D, R. (2018) The Climate of the Antarctic Peninsula during the Twentieth Century: Evidence from Ice Cores. DOI: 10.5772/intechopen.81507.
- Turner J, Colwell SR, Marshall GJ, et al. (2005) Antarctic climate change during the last 50 years. *International Journal of Climatology* 25(3): 279-294.
- Turner J, Lu H, White I, et al. (2016) Absence of 21st century warming on Antarctic Peninsula consistent with natural variability. *Nature* 535(7612): 411-415.
- 685 Zhu J, Xie A, Qin X, et al. (2021) An Assessment of ERA5 Reanalysis for Antarctic Near-Surface Air Temperature. *Atmosphere* 12(2): 217.

690